UNITED NATIONS UNIVERSITY
GEOTHERMAL TRAINING PROGRAMME
Orkustofnun, Grensasvegur 9,
IS-108 Reykjavik, Iceland

Reports 2013
Number 34

DESIGN OF A COOLING SYSTEM FOR STORAGE OF AGRICULTURAL PRODUCTS WITH EMPHASIS ON IRISH POTATOES

Jane Uwera
Ministry of Infrastructure
EWSA – Energy, Water and Sanitation Authority
P.O. Box 537
Kigali
RWANDA
kamanzijn@yahoo.com

ABSTRACT

This project focuses on the design of a cooling system for storage of agricultural products. It compares the efficiency of a vapour compression cycle powered by electricity from a binary geothermal power plant, and an absorption refrigeration unit which uses a geothermal heat source to drive the absorption cycle in a chilling process, both in a 25°C environment with a compartment temperature of 5°C. These two cycles are to provide the same cooling to the cold storage with a heat load equivalent to 140 kW. The parameters that were mainly monitored for comparison are COP, the power required to run the cycles, and the required mass flow of a geothermal fluid. After mathematical and thermodynamic analysis of the cycles, it was found that the overall efficiency of a binary plant coupled to the compression refrigeration is a bit low, or 0.432, as it must include both the thermal efficiency of the plant and the COP of the compression cycle, and that of the absorption refrigeration cycle is 0.471, but can go as high as 0.6 when a heat exchanger is used.

1. INTRODUCTION

Geothermal energy is a sustainable form of energy that can be used directly as heat or indirectly by conversion to other forms of energy. The method of its utilization is highly dependent on thermodynamic properties and the fluid chemistry. The high temperature resources are mainly used for power generation while the lower temperature resources can be used partially for power generation and other direct use applications. Geothermal resources in the range of 80-150°C can preferably be used to power the heat driven processes, such as cooling systems, and in absorption refrigeration system which uses thermal energy as the heat source. Resources within this temperature range are probable to be found in Rwanda's geothermal fields. Karisimbi, which began drilling activities recently, is one of them.

Rwanda is an East African country located along the Western Branch of the East African Rift system with a surface area of 26,338 km^2 and a population estimate of 11 million inhabitants (NISR, 2012). Rwanda is an agricultural country with about 90% of the population engaged in subsistence agriculture, with few natural resources. The primary foreign exports are tea and coffee, while tourism is the third

largest source of foreign exchange. Irish potatoes are the most common food crop produced on large scale in the Northern Province where most of Rwanda's geothermal fields are located.

The term refrigeration refers to cooling of an area or a substance below the environmental temperature, and therefore involves the process of removing heat. Mechanical refrigeration uses the evaporation of a liquid refrigerant to absorb heat. The refrigerant goes through a cycle so that it can be re-used. The main cycles include vapour-compression, absorption, steam-jet of steam ejector, and air.

This report discusses the design of a cooling system for storage of agricultural products using geothermal energy, with a case study on the Karisimbi geothermal field, Rwanda.

1.1 Objective of the study

The purpose of this study is to assess two different refrigeration processes and model the systems by analysing the thermodynamic properties of the working fluids and setting up the cooling units. There are two well-known refrigeration systems which are vapour compression and vapour absorption cycles. Comparison of the performance of these two systems will be observed, operating from a proposed geothermal heat source. The vapour compression cycle will be integrated with a binary power plant for the supply of electricity to run the compressor motors while the vapour absorption cycle will be powered by the typical geothermal heat source.

2. GEOTHERMAL IN RWANDA

2.1 Geological and structural settings

Rwanda hosts two prospective areas: the National Volcanoes Park and the faults associated with the East African Rift near Lake Kivu. The National Volcanoes Park was identified as a potential host for large, high-temperature geothermal systems, while the rift provides an environment for small, low-to moderate-temperature resources. The current study involves the northwest part of Rwanda that includes the National Volcanoes Park. The main structural trends of this area are controlled by the older basement structures. The Nyiragongo volcano to the west of the area has been erupting periodically. This signifies that a heat source for a geothermal system could exist around the major volcanoes. The area of exploration is between Nyiragongo volcano to the west, Muhabura volcano to the east and Gisenyi to the south. The major structural trends, as summarized by the German Institute of Geosciences and Natural Resources (BGR, 2009), show that the older rift border faults have a predominantly northwesterly trend while the younger eastern rift border faults have a northeasterly trend. Other important structures include an accommodation zone, which marks the boundary between the basement rocks and volcanic rocks. It is anticipated that this structural pattern is probably buried below the younger volcanic rocks (Onacha, 2008).

2.2 Geothermal fields

The geothermal areas in the western region cover an area of about 900 km2 and it has been further sub-divided into the three regions of Karisimbi, Gisenyi and Kinigi. The Karisimbi geothermal prospect is found on the southern slopes of the Karisimbi Volcano. Karisimbi field is part of the National Volcanoes Park. No geothermal manifestations such as fumaroles or alteration have been reported in this area. However, a couple of hot springs are located south and out of the volcanic field, as shown in Table 1, with the highest temperature of 64°C at Karago (located in the southern part of Karisimbi geothermal prospect).

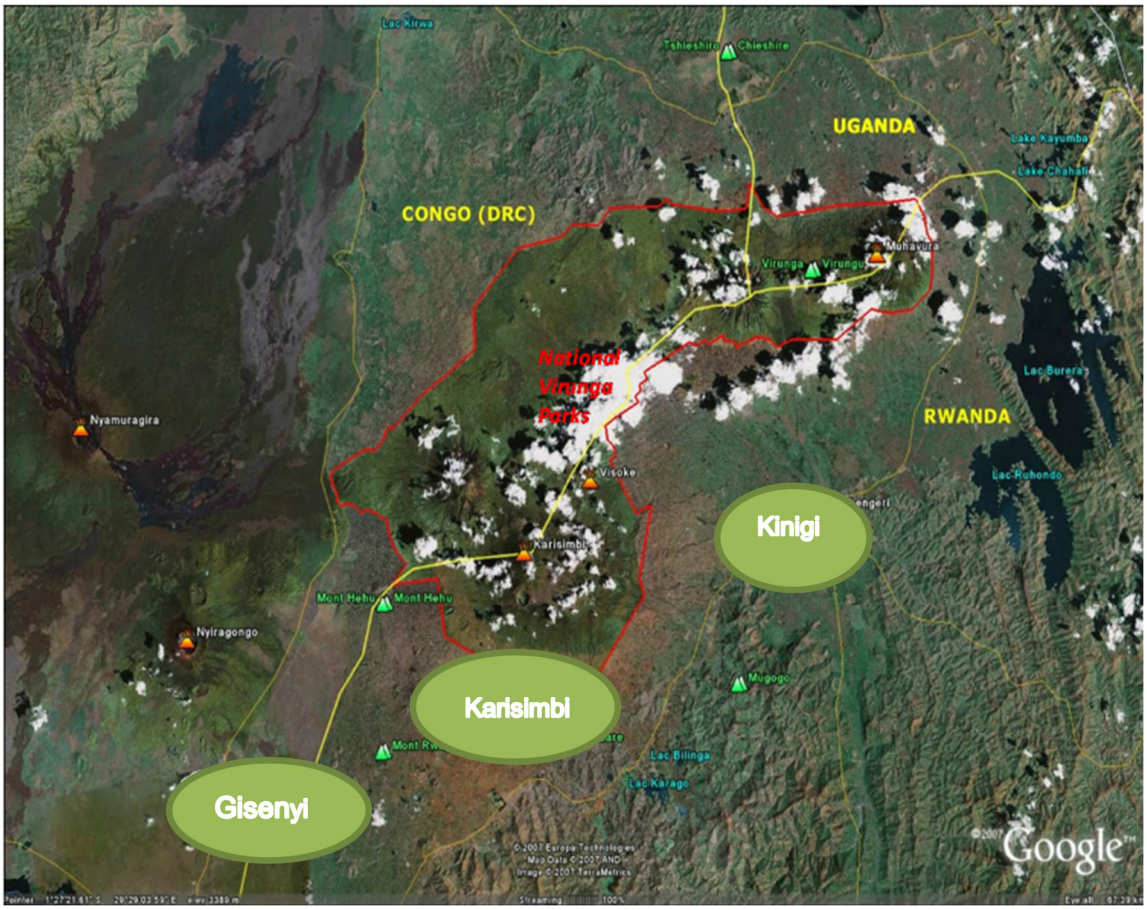

FIGURE 1: Map showing the geothermal fields in northwest Rwanda (modified from Namugize, 2011)

2.3 Karisimbi geothermal field

Karisimbi geothermal field is situated in the western province and occupies an area of about 200 km^2. The prospect lies to the south of the National Volcanoes Park (NVP). This area has very fertile soils suitable for agricultural activities, with a heavy downpour and an annual rainfall average of 800 mm. The proposed sites for exploration drilling are found to the north of Mukamira. The calculated temperature ranges from the geothermometers are very low (Table 1), probably due to the nephelinites absorbing silicate hot springs which produce sodium bicarbonate water with temperature between 70-75°C. The flow rates from all the vents are estimated to be 2-5 kg/s and are controlled by fractures. It is postulated that some of the vents could be buried below the lake's surface. Based on fluid geothermometers, the reservoir temperature is estimated to be between 150 and 210°C. (Newell et al., 2006; BGR, 2009).

TABLE 1: Surface temperatures and calculated temperature based on fluid chemistry

Location	Surface temp. (°C)	Quartz temp. (°C)	Na/K temp. (°C)	Temperature range (°C)
Karago	64	126	147	120-140
Gisenyi	70-72	107	175	105-210

Figure 2 shows the expected weather conditions in Karisimbi.

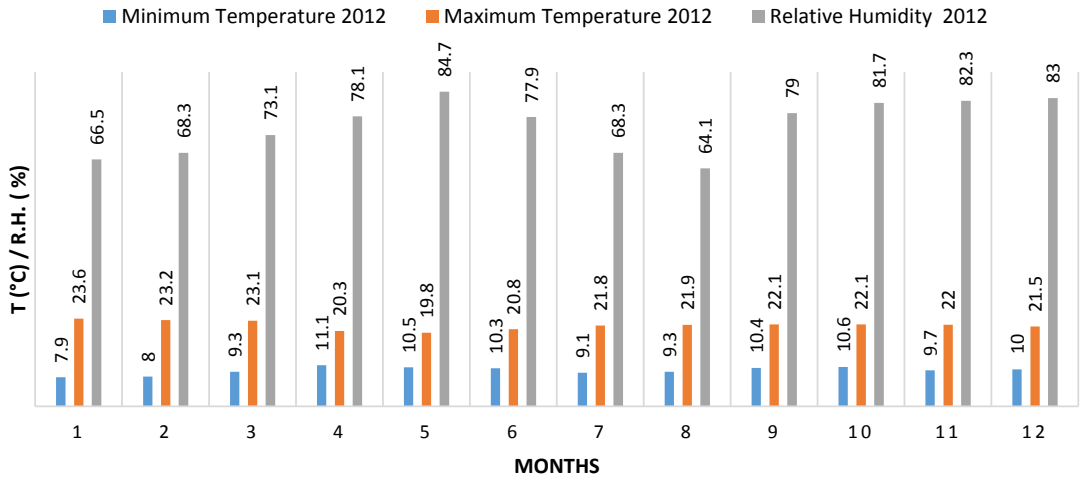

FIGURE 2: Weather conditions in Karisimbi in 2012 on a monthly basis

2.4 Geothermal utilization and direct use opportunities

The Government of Rwanda (GoR), through the Ministry of Infrastructure (MinInfra) and the newly formed Electricity Water and Sanitation Authority (EWSA), has plans to explore and develop over 300 MWe from geothermal resources by 2017. The immediate goal is the establishment of the viability of the geothermal resources by drilling wells in one of the geothermal prospects. Drilling operations for the three first exploration wells are now ongoing and the next three prospects will follow immediately. Rwanda has identified four geothermal prospects; once drilling is successful, the immediate plan is the connection of wellhead generating units for early power generation and feasibility studies for direct use applications of geothermal energy. The GoR also intends to develop direct utilization of geothermal resources in the agricultural sector using greenhouses, and drying rice and fish. Other direct uses will include the uses of geothermal heat in pyrethrum processing and for drying tea and coffee. Geothermal energy could also be used in industrial processes such as mineral processing and cooling systems applications (Onacha, 2011).

3. CASE STUDY ON IRISH POTATOES

3.1 Irish potatoes value chain in Rwanda

The potato has become an important food crop in Rwanda with about 133,000 hectares under cultivation; more than 1 million metric tonnes (MT) of potatoes are produced annually (Agri, 2012). The Irish potato requires a relatively cool and moist climate to achieve the best results. Musanze, Burera, Gicumbi and Nyabihu districts account for 90% of the national potato production in Rwanda. A significant portion of the Irish potatoes produced are consumed in the areas of production and there is no potato storage or processing in Rwanda yet. Most potatoes are transported to the markets almost immediately after harvest, generally unwashed in large bags. In most cases, the farmer does not know the price he will receive for his potatoes before reaching the main market; this becomes a challenge for them in terms of marketing and economic planning. The potatoe production and selling prices are summarized in Table 2.

TABLE 2: Potato production cost and selling prices in Rwanda

Potato	Size and units	Value
Production cost	USD/ha	1,068-2,595
Selling price	USD/kg	0.099-0.46
Average production cost	USD/kg	0.13
Average yield	kg/ha	9,400
Average crop value	USD/ha	1,277

3.2 Potato growing seasons

There are basically two seasons (A and B) for potato growing in Rwanda, as shown in Figure 3, with the first season (A) extending from September to December and the second season (B) extending from February to May.

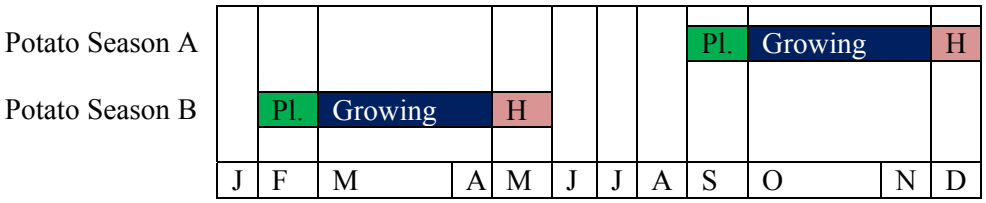

FIGURE 3: Potato growing seasons in Rwanda; **Pl** stands for planting, and **H** for harvesting

3.3 Statement of the problem and need for the study

The potato production cycle in Rwanda is quite short, about 3-4 months, and follows two main growing seasons (Figure3), however, in some regions it is possible to extend the growing cycle beyond those seasons if sufficient moisture is available in the soil. The lack of storage and processing facilities makes it necessary for Rwandan potato farmers to sell their produce almost as soon as it is harvested; this is the current weakness of the Rwanda potato sector. The big challenge is the lack of storage facilities for their produce on a large scale and leads to the immediate sale of most of the harvest to neighbouring countries like Burundi and others at low prices. Yet, if they had some storage facilities, potatoes could be stored for some time and sold at competitive prices.

3.4 Potato storage conditions

3.4.1 Mid and long-term storage

The objective of long-term storage is to maintain a consistent, ideal environment for the duration of the storage period. Long-term storage demands more critical control than short-term storage. Recommended storage temperatures depend upon crop condition, variety and intended end use. General recommendations for storage temperatures are listed in Table 3.

TABLE 3: Potential storage duration of potatoes

Potatoes	Temperature (°C)	RH (%)	Potential storage duration
Fresh market	4-7	95-98	10 months
Processing	8-12	95-98	10 months
Seeds	0-2	95-98	10 months

3.4.2 Storage design parameters and related heat load calculations

It is desired to design a cooling system for storage of agricultural products with an emphasis on potatoes. This storage is proposed to be built in the northern province of the country in the Musanze district near most of the geothermal fields in Rwanda, in order to make use of the geothermal heat. It has a capacity for storing 312 tonnes of potatoes, using wooden storage bins. The other detailed dimensions and conditions are summarized in the tables below along with the related refrigeration load calculations.

3.4.3 Refrigerated cold storage

Figure 4 shows the location of a cooling unit in the cold storage, together with the proposed wooden storage bins (Figure 5).

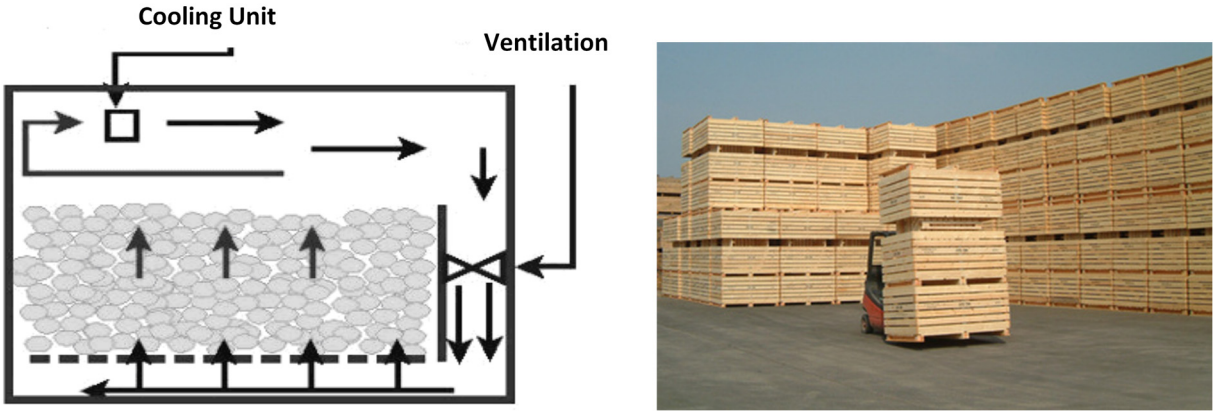

FIGURE 4: Cooling unit connected to cold store and proposed 1000 kg storage bins (PalletLink, 2013)

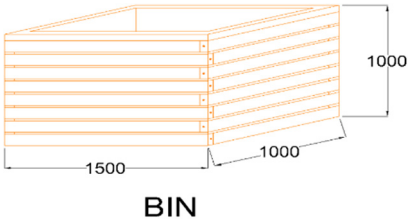

FIGURE 5: A potato storage bin

3.4.4 Wooden storage bins

The storage bins under this design (Figure 5) are made of cypress timber. The major advantages of wooden bins are low cost, superior strength, and having been the industrial standard for a long time. Wood bin kits are produced and assembled locally which minimizes transportation cost from manufacturer to end users. Their dimensions are summarized in Table 4.

TABLE 4: Wooden bin details

Wooden storage bins	Units	Value
Number of bins	Piece	312
Bin dimensions	m	L=1.5 ,W=1, H=1
Bin weight	kg	90
Total weight of bins	kg	28,080
Storage capacity of the bin	kg	1000
Specific heat of the bin	kJ/kg°C	0.5

3.4.5 Dimensions for potatoes cold storage

Many different things must be considered while planning the construction of cold warehousing facilities and it requires an enormous degree of precision and attention to details. One of the most important things to consider is which concrete floor to use. Not all concrete floors are made alike, and there are many different methods that can be used to install them. The chilled room must also consider the sealing system which best fits the needs of the cold storage and the corresponding concrete walls and roof. Homogeneous insulation is assumed. Enough space must be left above the storage bins for lights and other cooling system ducts. Table 5 shows the details of the cold room.

3.4.6 Description of storage construction materials and insulation

The insulation materials used are wood fibre, which includes residue and waste wood to produce a suitable low density wood fibre board which is easy, safe to work with and cost-effective. It is designed

to be used inside the building as it offers additional insulation when used in interior walls, floors and ceilings. Wood fibre insulation can absorb moisture and has high vapour diffusion capabilities, allowing the panels to act as a breathable structure. This helps to improve the indoor air quality by absorbing and releasing heat back later when the temperature decreases (see Figure 6 and Table 6 for working and storage conditions).

TABLE 5: Details of the cold room for potato storage

Potatoes	Units	Quantity
Storage capacity	bins	312
Store dimensions	m	L=25, W=16, H=5.5
Volume (V)	m^3	2,200
Surface area including the floor (A)	m^2	1,294
Temperature difference, ΔT	(°C)	20
Specific heat of potatoes	kJ/kg°C	0.82
Rate of respiration	W/kg	0.028
Overall coefficient of transmission	$W/m^2°C$	1.6

TABLE 6: Working conditions and assumptions for the design system; uniform insulation is assumed on the walls, ceiling and floor

Loading weight and time:	104 bins (104,000 kg of potatoes); 3 days to fill	
Cooling rate:	1st day , 20 to 10°C; 2nd day, 10 to 5°C	
Air changes from door opening during cooling	times per day	6
Air changes from door opening during storage °C	times per day	1.8
Heat load to lower air from 20 (90% RH) to 10°C (95% RH)	kW/m^3	0.45
Heat load to lower air from 10 to 5°C (95% RH)	kW/m^3	0.087

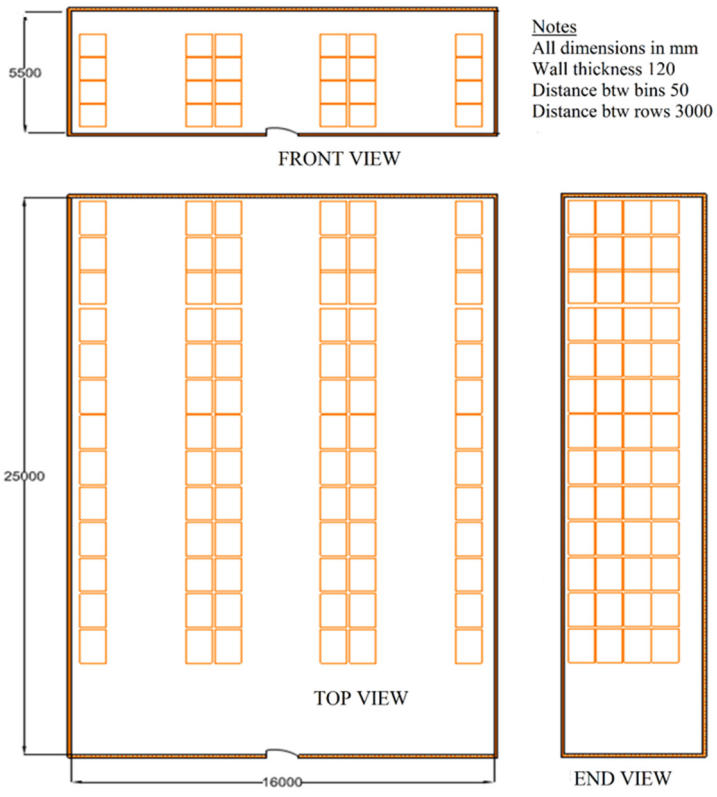

FIGURE 6: Overview of the bins in the chilled room

3.4.7 Storage heat load calculations

Heat load determination. The total heat load consists of the amount of heat to be removed from the refrigerated room during a certain period. It is dependent on two main factors: heat leakage or heat transfer load, and heat usage or service load, respectively. Thus, the following types of heat loads were considered in the design of this cold room.

Building transmission load. The building transmission load is the total amount of heat that leaks through the walls, windows, ceiling, and floor of the refrigerated room per unit of time (usually kW or kJ/s). Heat leakage, therefore, is affected by the amount of the exposed surface, thickness and the kind of insulation used, and the temperature difference between the inside and the outside of the refrigerated room. Thus, it is the heat transfer from the outside into the refrigerating space via the insulated walls of the refrigerator:

$$Building\ transmission\ load = A * U * \Delta T \quad (1)$$

where A = The outer surface area of the building (m^2);
U = The overall coefficient of transmission (W/ m^2°C); and
ΔT = The temperature difference (°C).

Air change heat load. Air that enters a refrigerated space must be cooled. Air needs to be renewed, and consequently there is a need for ventilation. When air enters the refrigerated space, heat must be removed from it. Air which enters the refrigerated space usually cools and reduces in pressure. If the refrigerated room is not air tight, air will continue to leak in. Also, each time a service door or walk-in door is opened, the cold air inside, being heavier, will spill out the bottom of the opening, allowing the warmer room air to move into the refrigerated room. The actions of moving materials in or out of the refrigerated room, and a person going into or leaving the refrigerated room, result in warm air moving into the refrigerated space through the process of air infiltration. Hence, the air change heat load is the heat transfer due to closing and opening of the refrigerator doors and subsequent changes in the air-heat content in the refrigerated space.

$$ACL = V_s * \rho(h_o - h_i) * ACD \quad (2)$$

where ACL = Air change load due to door opening, infiltration and ventilation etc. (kW);
V_s = Volume of the cold room (m^3);
h = Enthalpy of air (kJ/kg);
ρ = Density of air (kg/m^3);
ACD = Air change per day, number of times; and
Subscripts o and i denote out and in, respectively.

Miscellaneous heat loads. All sources of heat not covered by leakage, product cooling, and respiration load are usually listed as miscellaneous loads. Some of the more common miscellaneous loads are lights, electric motors and people. These are small loads estimated to be 4,4 kW in total.

Product heat load. Any substance that is warmer than the refrigerator is placed where it will lose heat until it cools to refrigerator temperature. Respiration heat is the heat given off by living things, especially plant products, in this case potatoes. Potato tubers from immature lands are susceptible to bruising and skinning which can have high respiration rates. The use of a cooler temperature and/or higher air inflow is an effective method for improving their conservation. The respiration rate of potatoes is shown in table 7 (Trevor et al., 2013).

TABLE 7: Heat load calculations

Temperature (°C)	**ml CO_2 /kg·h**	**Average respiration rate (W/kg)**
5	6-8	0.000336
10	7-11	0.000432
15	7-16	0.000552
20	9-23	0.000768

$$PHL = W * c_p * \Delta T/t \quad (3)$$

where PHL = The product heat load (kW);
W = The potato weight (kg); and
c_p = The specific heat of potatoes (kJ/kg °C).

3.5 Heat usage load

The heat usage or service load is the sum of the following heat loads per unit of time: cooling the content of the refrigerated room temperature, cooling of air changes, removing respiration heat from potatoes, removing heat released by electric lights, electric motors, and the like, and heat given off by people entering and/or working in the refrigerated room. Usage, or the service load of the refrigerated room, was determined by the temperature of the articles that were put into the refrigerator, their specific heat, generated heat, and latent heat as the requirement demanded. Another consideration is the nature of the

service required. This involved air changes (determined by number of times per day that the doors of the refrigerator would be opened) and the heat generated inside by fans, lights and other electrical devices.

Heat load calculations are divided into two cases: consideration of the peak refrigeration load, especially in filling up and empting the store, and consideration of the heat load when the room has attained the room storage temperature.

3.5.1 Scenario A (peak refrigeration)

The storage room took 3 days to fill and the temperature was reduced as shown in Table 8 to reach storage room temperature (20-10-5°C).

TABLE 8: Peak refrigeration load capacity

Parameter	Value (kW)
Building transmission load	11.5
Air change load from door openings	10.2
Product cooling	71.2
Miscellaneous heat loads	4.4
Heat of respiration during cooling potatoes	24.5
Maximum heat accumulated in storage before cooling completed	4.9
Subtotal	126.7
Design margin (10%)	12.6
Total required refrigeration	**140**

The total heat load calculated for the chilled room is 140 kW**.**

3.5.2 Scenario B (Storage temperature)

The total refrigeration for a completely chilled storage room is 34 kW as shown in Table 9.

TABLE 9: Storage temperature refrigeration load capacity

Parameter	Value (kW)
Building transmission load	11.6
Air change load from door openings	3
Miscellaneous heat loads	4.4
Respiration rate	12
Subtotal	31
Design margin 10%	3.1
Total required refrigeration	**34**

Scenario A (peak refrigeration) operates at 140 kW while scenario B needs 34 kW, which is the load after the room has reached a constant temperature.

4. THEORY OF REFRIGERATION SYSTEMS

A refrigeration is a process of removing heat from one location, mainly in a confined space, and rejecting the unwanted heat into a specific preferable environment; in other words, the refrigeration process is a

method for lowering the temperature of an object. There are two common refrigeration systems that are widely used: vapour Absorption Refrigeration Systems (ARS) and vapour Compression Refrigeration (CR) systems. This project will mainly focus on the comparison between these two cycles by evaluating their efficiency (Table 10).

TABLE 10: Absorption system compared to compression system

	Absorption	Compression
A	Uses low-grade energy like heat. Therefore may be worked on exhaust system from I.C. engines, etc.	Uses high-grade energy like mechanical work
B	Moving parts are only in pump which is a small element of the system. Hence operation is smooth.	Moving parts are in compressor, therefore, more wear, tear and noise
C	The system can work on lower evaporator pressures also without affecting the COP	The COP decreases considerably with decrease in evaporator pressure
D	No effect of reducing the load on performance	Performance is adversely affected at partial-loads
E	Liquid traces of refrigeration present in piping at the exit of evaporator constitute no danger	Liquid traces in suction line may damage the compressor
F	Automatic operation for controlling the capacity is easy	Is difficult

4.1 Vapour absorption cycle

Absorption refrigeration systems are much like vapour compression cycles but the compressor is replaced by a generator and the absorber (Figure 7). Refrigerant enters the evaporator in the form of a cool, low-pressure mixture of liquid and vapour (4). Heat is transferred from the relatively warm water to the refrigerant, causing the liquid refrigerant to boil. The absorber draws in the refrigerant vapour (1) to mix with the absorbent. The pump pushes the mixture of refrigerant and absorbent up to the high pressure side of the system. The generator delivers the refrigerant vapour (2) to the rest of the system. The refrigerant vapour (2) leaving the generator enters the condenser, where heat is transferred to water at lower temperature, causing the refrigerant vapour to condense into a liquid. This liquid refrigerant (3) then flows to the expansion device, which creates a pressure drop that reduces the pressure of the refrigerant to that of the evaporator. The resulting mixture of liquid and vapour refrigerant (4) travels to the evaporator to repeat the cycle.

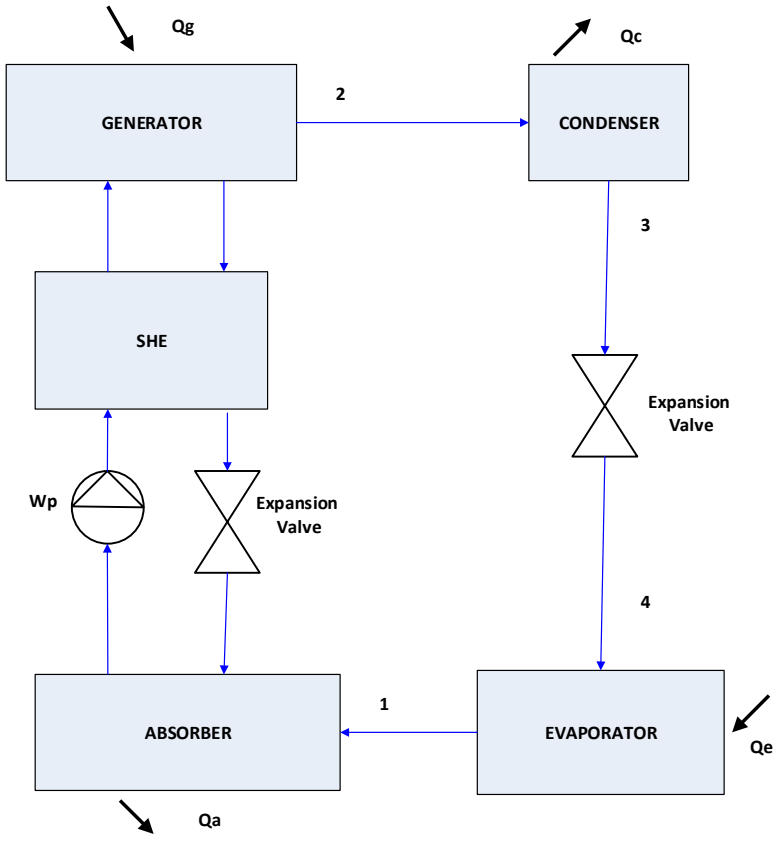

FIGURE 7: Schematic diagram of a simple absorption refrigeration system

4.1.1 Principle of operation

The most common principle of operation for a simple absorption system is based on principles first developed by the French scientist Ferdinand Carré (about 1860). More details on absorption systems were given by Nibergall (1959), Bäckström (1970) and ASHRAE (1996). As a vapour compression system, an absorption system of this type consists of the following components (Figure 8):

Condenser	Where the refrigerant is condensed to liquid
Expansion valve	Where the pressure of the refrigerant liquid is reduced from condensing pressure to the pressure in the evaporator
Evaporator	Where the refrigerant evaporates, for which process heat is supplied – from the compartment/room to be cooled

Instead of a mechanically operated compressor in the vapour compression cycle, the absorption system has a "*thermal compressor"* involving the following components:

Absorber	Where the refrigerant vapour is absorbed, and forms a *liquid* solution. During this process, heat is released, which means that the absorber must be cooled. The heat released is equivalent to the heat of condensation plus a heat of solution (or mixing) pertinent to the combination of refrigeration and the absorption medium.
Pump	By which the solution leaving the absorber is given a pressure equivalent to the pressure in the generator (same as in the condenser).
Generator	Where the refrigerant is separated from the solution by a distillation process. In a simple case, this is done by just "boiling" off the refrigerant from the solution. Heat (equal to the operating energy of the system) must be supplied for this process.
Regulating valve	Where the "poor" solution from the generator is passing on its way from the generator to the absorber. The valve is necessary since the pressures in these two components are different.

In order to decrease the demand for operating heat, and thus improve the efficiency, it is beneficial to use a heat exchanger, where heat is recovered from the hot "poor" solution leaving the generator, and used for preheating the "rich" solution from the absorber before it enters the generator.

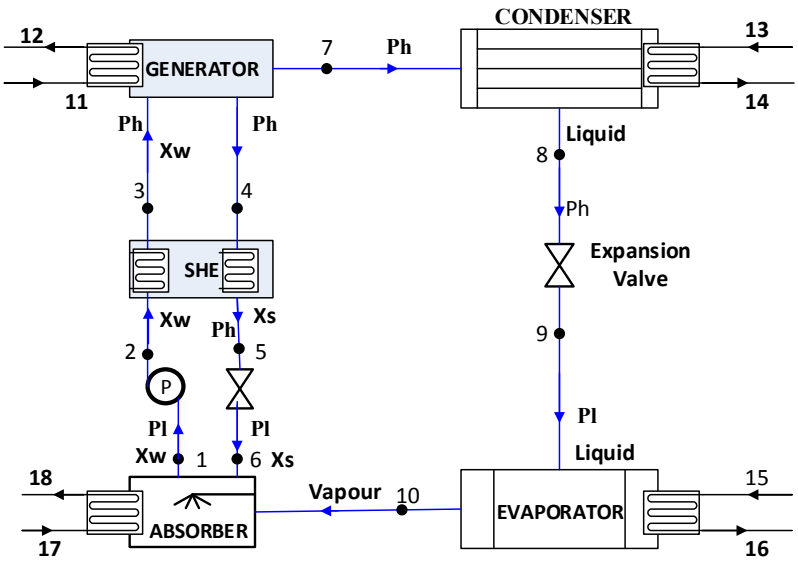

FIGURE 8: NH3-H2O absorption refrigeration system

4.1.2 System efficiency and coefficient of performance

Efficiencies of absorption chillers are described in terms of coefficient of performance (COP), which is defined as the refrigeration effect divided by the net heat input. Single-effect absorption chillers have COPs of approximately 0.6-0.8 out of an ideal 1.0. Since the COPs are less than one, the single-effect chillers are normally used in applications that recover waste heat, such as waste steam from power plants or boilers. Double-effect absorption chillers have COPs of approximately 1.0 out of an ideal 2.0. While not yet commercially available, prototype triple effect absorption chillers have calculated COPs of 1.4 to 1.6 (Southern California Gas Company New Buildings Institute, 1998).

Compared with mechanical chillers, absorption systems have a low coefficient of performance. However, absorption chillers can substantially reduce operating costs because they are powered by low-grade waste heat.

It is recommended to use a solution heat exchanger in absorption systems as it allows the solution from the absorber to be preheated before entering the generator by using the heat from the hot solution leaving the generator. Therefore, the COP is improved as the heat input at the generator is reduced.

Moreover, the size of the absorber can be reduced as less heat is rejected. Experimental studies show that the COP can be increased up to 0.6 when a solution heat exchanger is used.

The temperature of the heat source is the most important factor in the thermal efficiency of an absorption chiller. The higher the temperature of the heat source, the better the COP. Also, the efficiency of an absorption machine quickly deteriorates as soon as the temperature of the heat source drops below the design figure.

Efficiency of an absorption refrigeration system can be expressed by the coefficient of performance (COP), which is defined as the ratio between the amounts of heat/energy absorbed from the environment by the evaporator and the heat/energy supplied to the generator to operate the cycle.

$$COP = \frac{Cooling\ capacity\ (Q_e)}{Heat\ used\ to\ drive\ the\ chiller\ (Q_g)} \quad (4)$$

4.1.3 Working media

There are several refrigerant compounds that are usually used in refrigeration systems, but the most common are H_2O/NH_3 and $LiBr/H_2O$. $LiBr/H_2O$ is mainly used in cooling/air conditioning applications where the temperature goes as low as 0°C. $LiBr/H_2O$ is then used as the absorbent, and water as the refrigerant (Ratlamwala et al., 2012).

Aqueous Lithium Bromide is a salt solution substance where the salt component will start to precipitate when the mass fraction of the salt exceeds the maximum allowable solution solubility. Since the temperature and the mass fraction of the solution impact the solution solubility more than the pressure, these two components will affect the crystallization process significantly. Most of the available literature (e.g. ASHRAE Handbook of Fundamentals etc.) provides crystallization behaviour down to only 10°C. The typical evaporating temperature for an absorption chiller system is usually lower than 10°C. Hence, it is essential to have an accurate prediction of the crystallization temperature in this range during the design phase in order to avoid crystallization.

In the H_2O/NH_3 solution, NH_3 is the refrigerant in the mixture. It has a freezing point of -77°C and has high latent heat from vaporization. In this report, H_2O/NH_3 is used for absorption cycle applications as it has a low freezing point, and is low in cost (Srikhirin et al., 2001).

Ammonia is toxic, gaseous, an irritant, and is corrosive to copper alloys. With an ammonia refrigerant, the ever present risk of an escape brings with it a risk to life. However, data on ammonia escapes have shown this to be an extremely small risk in practice; consequently, there is no control on the use of ammonia refrigeration in densely populated areas and buildings in almost all jurisdictions in the world. However, in most cases, a secondary circuit with glycol to transport heat from the cooled storage to the working fluid is employed, so that leakages will not come in contact with the stored goods.

Due to the working principle of the absorption refrigeration cycle a pair of media is needed. The traditional combination is the pairing of ammonia and water, the ammonia being the refrigerant and water the absorption medium. The essential reasons for why this pair is suitable to use are the facts that ammonia is a good refrigerant and that the saturation vapour pressure of ammonia in a water solution is

considerably lower than that of pure ammonia (refer to Appendix I, Figure 1). The pairing of ammonia and water has interesting thermodynamic properties: both fluids have good heat transfer characteristics. One drawback, however, is that the vapour formed in the generator contains not only ammonia, but also, to certain extent, water vapour. In order to decrease the water content in the refrigerant, a "water separator", or rectifier, is installed along with the generator. In large plants, the generator is designed as a distillation column.

4.1.4 Necessary conditions for the selection of working fluids

The performance of the cycle depends mainly on the chemical and thermodynamic properties of the working fluids. The following elements influence the performance of the working fluid:

- Refrigerant should have high vaporization heat, and a high concentration within the absorbent in order to maintain a low circulation rate between the generator and the absorber per unit of cooling capacity;
- It is recommended that the fluid be chemically stable, non-toxic and non-explosive;
- The liquid phase must have a margin of miscibility within the operating temperature range of the cycle;
- The difference in boiling temperature between the pure refrigerant and the mixture at the same pressure should be as large as possible;
- Properties such as viscosity, thermal conductivity, and the diffusion coefficient should be taken into account; and
- Refrigerant and absorbent should be non-corrosive, environmental friendly and low in cost.

4.1.5 Thermodynamic analysis of the system

A schematic of a typical water–ammonia absorption refrigeration system is illustrated in Figure 8. The system includes a generator, absorber, condenser, evaporator, and a solution heat exchanger. The determination of the thermodynamic properties of each state point in the cycle, the amount of heat transfer in each component, and the flow rates at different lines depend on the generator temperature, evaporator temperature, condenser temperature, absorber temperature, liquid-liquid heat exchanger effectiveness, and the refrigeration load.

For carrying out a thermodynamic analysis of the proposed vapour absorption refrigeration system, the following assumptions were made:

- No pressure changes except through the flow pump and pressure expansion valve.
- At point 1, 4 and 8, there is only saturated liquid.
- At point 10, there is only saturated vapour. Pumping is isentropic. Assume a weak solution contains a larger percentage of refrigerant and a smaller percentage of absorbent and a strong solution contains a larger percentage of absorbent and a smaller percentage of refrigerant. The percentages of the weak solution at state 1, 2 and 3 and the percentages of the strong solution at state 4, 5 and 6 will remain same. The temperatures at thermodynamic states 11, 12, 13, 14, 15, 16, 17 and 18 are the external circuit for water which is used to input heat for the components of the system shown in Figure 8.
- This system has two pressure limits; one is a high-pressure limit and the other is the low-pressure limit.
  P1 = P6 = P9 = P10 = Low pressure.
  P2 = P3 = P4 = P5 = P7 = P8 = High pressure.

Energy analysis

Generator:
On balancing the energy across the generator:

$$Q_g + Q_3 = Q_4 + Q_7 \quad (5)$$

And:

$$Q_3 = \dot{m}_3 * h \quad (6)$$

$$Q_4 = \dot{m}_4 * h_4 \quad (7)$$

$$Q_7 = \dot{m}_7 * h_7 \quad (8)$$

where Q = Heat flow (kW);
$\dot{m}$ = Mass flow (kg/s);
h = Enthalpy (kJ/kg).

Balancing the concentration across the generator:

$$\dot{m}_3 * X_3 = \dot{m}_4 * X_4 + \dot{m}_7 * X_7 \quad (9)$$

$$\dot{m}_1 = \frac{\dot{m}_4 * X_s}{X_w} \quad (10)$$

where X = Ammonia content in working media.

Combining Equations 9 and 10:

$$\dot{m}_6 = \frac{-\dot{m}_{10}}{1 - \frac{X_6}{X_1}} \quad (11)$$

Using Equations 6-8:

$$Q_g = (\dot{m}_7 * X_7) + (\dot{m}_4 * X_4) - (\dot{m}_3 * X_3) \quad (12)$$

Heat supplied to the generator is:

$$Q_g = \dot{m}_6 * C_{p_{water}} = \pi r^2 * (T_{12} - T_{11}) \quad (13)$$

$$\dot{m}_{11} = \frac{(\dot{m}_7 * X_7) + (\dot{m}_4 * X_4) - (\dot{m}_3 . X_3)}{C_{p_{water}} * (T_{12} - T_{11})} \quad (14)$$

Condenser:
On balancing the energy across the condenser:

$$Q_c + Q_8 = Q_7 \quad (15)$$

$$Q_8 = \dot{m}_8 * h_8 \quad (16)$$

$$Q_7 = \dot{m}_7 * h_7 \quad (17)$$

$$Q_c = (\dot{m}_7 * h_7) - (\dot{m}_8 * h_8) \quad (18)$$

Heat supplied to the condenser is:

$$Q_c = \dot{m}_{15} * C_{p_{water}} (T_{15} - T_{16}) \quad (19)$$

On comparing Equations 12 and 13, we can get m_{15}:

$$\dot{m}_{15} = \frac{(\dot{m}_7 * h_7) - (\dot{m}_8 * h_8)}{C_{p_{water}} (T_{15} - T_{16})} \quad (20)$$

Evaporator:
On balancing the energy across the evaporator:

$$Q_e + Q_9 = Q_{10} \tag{21}$$

$$Q_9 = \dot{m}_9 * h_9 \tag{22}$$

$$Q_{10} = \dot{m}_{10} * h_{10} \tag{23}$$

On putting the energy values for points 9 and 10 into Equation 21:

$$Q_e = (\dot{m}_{10} * h_{10}) - (\dot{m}_9 * h_9) \tag{24}$$

Knowing that heat extracted from the evaporator is:

$$e = \dot{m}_{17} * C_{p_{water}} * (T_{18} - T_{17}) \tag{25}$$

Comparing Equations 17 and 18:

$$\dot{m}_{17} = \frac{(\dot{m}_{10} * h_{10}) - (\dot{m}_9 * h_9)}{C_{p_{water}} * (T_{18} - T_{17})} \tag{26}$$

Absorber:
On balancing the energy across the absorber:

$$Q_a + Q_1 = Q_6 + Q_{10} \tag{27}$$

And:

$$Q_1 = \dot{m}_1 * h_1 \tag{28}$$

$$Q_6 = \dot{m}_6 * h_6 \tag{29}$$

$$Q_{10} = \dot{m}_{10} * h_{10} \tag{30}$$

We have already found out m_1 and m_6 by using Equations 10 and 11 for calculating T_5; we can use the relation of effectiveness of the heat exchanger:

$$T_5 = -\varepsilon - \frac{T_4}{(T_4 - T_2)} * (T_4 - T_2) \tag{31}$$

Using Equations 21-23, we can get Q_1, Q_6 and Q_{10}.

By putting energy values for 1, 6 and 10 into Equation 21, we get:

$$Qa = (\dot{m}_6 * h_6) + (\dot{m}_{10} * h_{10}) - (\dot{m}_1 * h_1) \tag{32}$$

We also know that the heat transfer from the absorber is:

$$Q_a = \dot{m}_{13} * C_{p_{water}}(T_{14} - T_{13}) \tag{33}$$

On comparing Equations 26 and 27, we can get m_{13}; similarly by using the energy balance, we can get:

$$\dot{m}_{13} = \frac{(\dot{m}_6 * h_6) + (\dot{m}_{10} * h_{10}) - (\dot{m}_1 * h_1)}{C_{p_{water}} * (T_{14} - T_{13})} \tag{34}$$

Heat exchanger:
The requirement of the heat exchanger area for the absorption system was calculated using the log mean temperature difference method. Since the rate of heat transferred is a linear function of the overall coefficient of heat transfer, the heat transfer area of the heat exchanger and the log mean temperature difference for the heat transfer process could be derived from Equation 29:

$$Q = U * A * LTMD \tag{35}$$

$$LMTD = \frac{(T_4 - T_3) - (T_5 - T_2)}{ln\left(\frac{(T_4 - T_3)}{(T_5 - T_2)}\right)} \tag{36}$$

Heat exchange efficiency becomes:

$$\eta_{she} = ln\left(\frac{(T_4 - T_3)}{(T_5 - T_2)}\right) \tag{37}$$

$$\dot{m}_4(T_4 - T_5) = \dot{m}_2(T_2 - T_3) \tag{38}$$

4.2 Vapour compression cycles

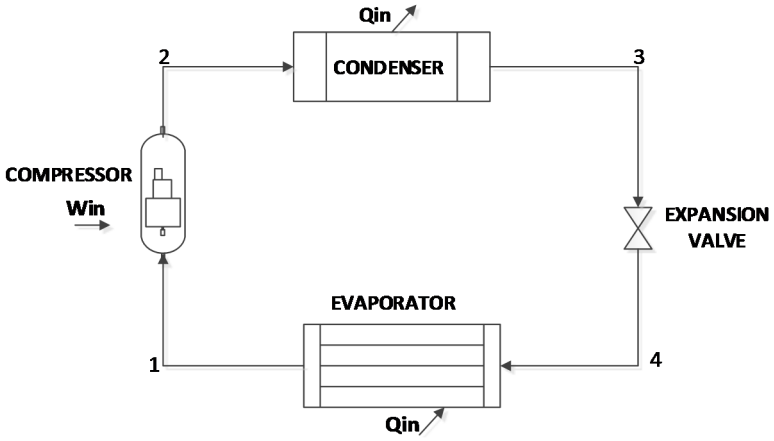

FIGURE 9: Schematic diagram of a simple compression refrigeration system

In the vapour-compression refrigeration cycle (Figure 9), refrigerant enters the evaporator in the form of a cool, low-pressure mixture of liquid and vapour (4). Heat is transferred from the relatively warm air or water to the refrigerant, causing the liquid refrigerant to boil. The resulting vapour (1) is then pumped from the evaporator by the compressor, which increases the pressure and temperature of the refrigerant vapour. The hot, high-pressure refrigerant vapour (2) leaving the compressor enters the condenser where heat is transferred to ambient air or water at a lower temperature. Inside the condenser, the refrigerant vapour condenses into a liquid. This liquid refrigerant (3) then flows through the expansion valve, which creates a pressure drop that reduces the pressure of the refrigerant to that of the evaporator. At this low pressure, a small portion of the refrigerant boils (or flashes), cooling the remaining liquid refrigerant to the desired evaporator temperature. The cool mixture of liquid and vapour refrigerant (4) travels to the evaporator to repeat the cycle.

Figure 10 shows in few steps how a compressor systems work. The process from 1 to 2 is when the compressor increases the pressure of the evaporated refrigerant vapour to raise its temperature. On the suction side, the compressor keeps the pressure of the liquid refrigerant low, causing the refrigerant to operate at a lower temperature. In the following step, from 2 to 3, the fluid enters the condenser and heat is rejected while the pressure stays constant. From 3 to 4 an expansion occurs under a throttling process where the enthalpy is constant. The pressure drops down as well as the temperature of the refrigerant. The final step is from 4 to 1. When the cold liquid enters the evaporator, heat is added and the liquid evaporates. This is the part where the cooling takes place (Wulfinghoff, 1999). In Figure 10, the relationship between temperature and entropy is shown in different positions in the compression cycle where the curve shows saturation for the working fluid.

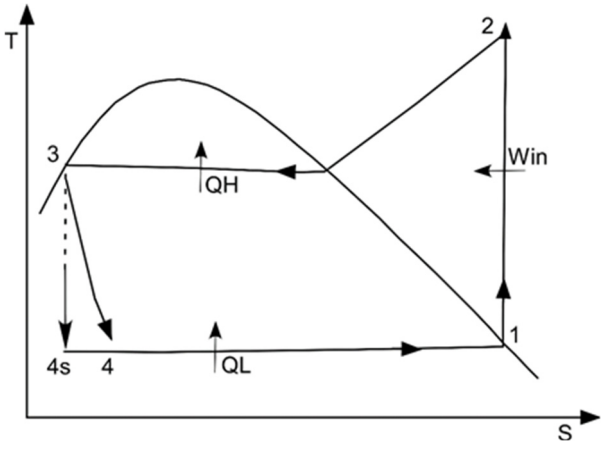

FIGURE 10: T-S diagram for a simple compression system

4.2.1 Analysis of the cycle

The thermodynamic analysis of the compression cycle is performed using the following assumptions:

a) The system is in steady state;
b) The vapour is saturated at the inlet of the compressor;
c) The isentropic efficiency of the compressor is 75%; and
d) There is no pressure loss along the pipe and in the valves.

Table 11 shows the mass and energy balance of the compression refrigeration system.

TABLE 11: Mass balance and energy balance of a vapour compression refrigeration system; refer to Figure 9 for orientation

Component	Mass balance	Energy balance
Compressor	$\dot{m}_1 = \dot{m}_2$	$W_{comp} = \dot{m}_1 h_1 - \dot{m}_2 h_2$ $W_{comp\ isent} = \dot{m}_1 (h_{isent} - h_1)$
Condenser	$\dot{m}_2 = \dot{m}_3$	$Q_{cond} = \dot{m}_2 h_2 - \dot{m}_3 h_3$
Expansion valve	$\dot{m}_3 = \dot{m}_4$	$h_3 = h_4$
Evaporator	$\dot{m}_4 = \dot{m}_1$	$Q_{ev} = \dot{m}_1 h_1 - \dot{m}_4 h_4 = (refrigeration\ effect)$

The technology in this cycle uses electricity to compress the working fluid and the cycle is relatively effective. The coefficient of performance (COP), as a measure of system efficiency, is defined as the ratio between the amounts of heat absorbed in the evaporator to the power given to the compressor:

$$COP_C = \frac{Cooling\ capacity}{Required\ input} = \frac{Q_E}{W_c} \quad (39)$$

where W_c = The work input into the compressor.

4.2.2 Refrigerant selection criteria

Selection of refrigerant for a particular application is based on the following requirements:

- Thermodynamic and thermo-physical properties;
- Environmental and safety properties; and
- Economics.

4.2.3 Thermodynamic and thermo-physical properties

The requirements are:

- *Suction pressure:* At a given evaporator temperature, the saturation pressure should be above atmospheric pressure to prevent air or moisture ingression into the system and for ease of leak detection.
- *Discharge pressure:* At a given condenser temperature, the discharge pressure should be as small as possible to allow light-weight construction of the compressor, the condenser, etc.
- *Pressure ratio:* Should be as small as possible for high volumetric efficiency and low power consumption.
- *Latent heat of vaporization:* Should be as large as possible so that the required mass flow rate per unit cooling capacity will be small.

4.2.4 Choice of refrigerant R134a

The refrigerant R134a was selected to be used in the proposed vapour compression cycle for the following reasons: It is an almost odourless liquid with a low boiling point of -26°C at atmospheric pressure. It has a low specific volume of vapour with a good volumetric efficiency. It is non-toxic, non-corrosive, and non-flammable. Its ozone depletion potential is zero with little global warming potential. More importantly, its cost is comparatively low, and it produces a relatively good refrigerating effect at moderate and economical operating conditions. Also, its leakage can be easily detected by using a soap solution.

5. THE BASIC CONCEPT OF ENERGY CONVERSION IN AN ORGANIC RANKINE CYCLE POWER PLANT

The simple organic Rankine cycle power plant follows the scheme shown in Figure 11. The working fluid is an organic fluid, also called refrigerant.

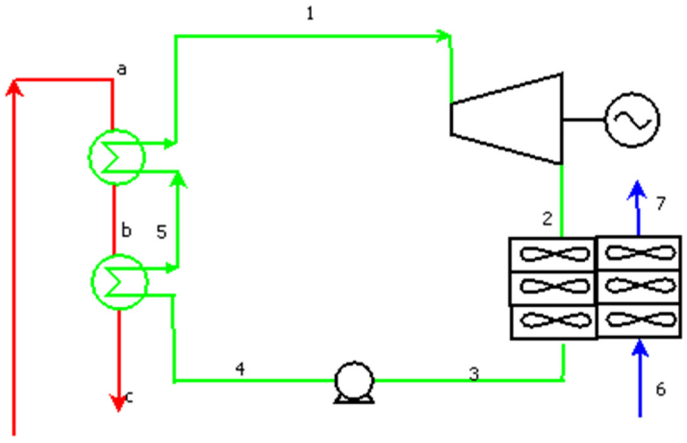

FIGURE 11: Simplified schematic of basic ORC power plant

5.1 The simplified schematic basis of ORC power plant

The geothermal fluid heat enters the system through a series of heat exchangers, in which heat is transferred to the working fluid. Typically, there are two stages of heat exchange: one occurring in a preheater, where the temperature of the working fluid is raised to its bubble point, and the other in an evaporator, where the working fluid is vaporized. However, in cases where the fluid must reach a superheated state, a third heat exchanger – a super heater – is added. After isobaric heat addition, which occurs between states 5 and 1, high-pressure vapour is expanded in the turbine (1-2). The exhaust vapour of the organic fluid from this process is superheated, which is a result of the characteristic retrograde shape of the working fluid saturation line. The superheated stream of the exhaust gas may be sent directly to the condenser where it is cooled to T_3 and condensed. However, if economically feasible, exhaust from the turbine may lead to another heat exchanger-regeneration which recovers part of the sensible heat. . After leaving the condenser, the working fluid enters the pump, where its pressure is increased to P4 and is returned directly, or through the regenerator, to the preheater. The working fluid operates in a sealed, closed-loop cycle. The thermodynamic process undergone by the working fluid is shown in commonly used temperature-entropy and pressure-enthalpy diagrams (Lukawski, 2009) in Figure 12.

Preheater and evaporator:
The analysis for the above two components are well described in many engineering books. Standard methodology assumes:

1. Steady state operating conditions;
2. No heat losses from heat exchangers not connected with the transfer of mass;
3. Pure concentration flow in heat exchangers;
4. Constant overall heat transfer coefficient;
5. Constant specific heat of heat source fluid; and
6. Changes of kinetic and potential energy of fluid is negligible.

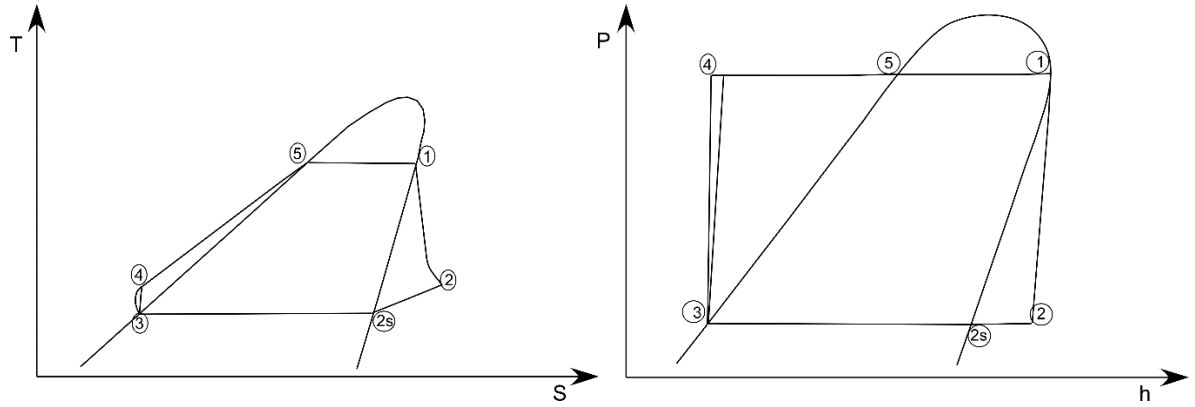

FIGURE 12: Temperature–entropy and pressure–enthalpy diagrams for a binary power plant

As heat losses in heat exchangers are neglected, the amount of heat added to the working fluid is equal to the heat extracted from the heat source.

$$Q = \dot{m}_{hs}(h_{hs,ev,in-}h_{hs,ph,out}) \tag{40}$$

$$Q = \dot{m}_{wf}\left(h_{wf,ev,out} - h_{wh,ph,in}\right) \tag{41}$$

where the subscript 'hs' refers to heat source fluid, "wf" to working fluid, "ph" to preheater and "ev" to evaporator.

In the temperature-heat exchange diagram of a heat exchanger, the place where the minimum temperature difference between two fluids occurs is called the pinch. The location of the pinch point and the value of the pinch point temperature is one of the major parameters influencing the performance of ORC power plants and will be investigated and optimized in this study.

Turbine:
The purpose of the turbine is to change the potential of pressurized gas into rotational kinetic energy. The stream of high-pressure vapour of an organic fluid expands in the turbine, causing its internal parts to rotate. The rotor is connected by a shaft to the generator which changes rotational kinetic energy into electricity. The expansion process is considered adiabatic and a steady state of operation is assumed. Knowing the isentropic efficiency of the turbine (η_t), which is given by the manufacturer, the generated power can be calculated as follows (DiPippo, 2008).

$$W_{gen} = \dot{m}_{wf}(h_1 - h_2) = \dot{m}_{wf}\,\eta_t(h_1 - h_{2s}) \tag{42}$$

where η_t is the isentropic efficiency of the turbine and state $2s$ corresponds to an ideal isentropic turbine.

The heat dissipation system is of great importance for binary power plants because of significantly bigger quantities of rejected heat per unit of electricity output compared to other sources of energy, as well as the high sensitivity for temperature variations of the heat sink. The heat dissipated from the cycle is primarily heat from condensation of the working fluid and can be defined in terms of the thermal efficiency of the cycle as:

$$Q_{rej} = Q_{in}(1 - \eta_{th}) \tag{43}$$

Where Q_{in} is the heat input to the cycle, in this case, the sum of the heat rates of the preheater and the evaporator, and η_{th} stands for the thermal efficiency of the cycle. The amount of heat that has to be rejected to the atmosphere per unit of work output is:

$$Q_{rej} = \frac{W(1 - \eta_{th})}{\eta_{th}} \tag{44}$$

where W = Power generated by the turbine.

Cooling tower:
To improve the net power output of the plant, it is very important to develop a cooling system that cools the steam leaving the turbine. This system is composed of an air cooled surface condenser which condenses the working fluid before it enters the pump. While transferring heat to the cooling air, the working fluid changes phase, from gaseous to liquid. The power consumed by the cooling tower fan is given by:

$$W_{fan} = \frac{V_{air} * \Delta p}{\eta_{fan}} \tag{45}$$

where V_{air} = Volumetric flow of the air through the fan;
Δp = Pressure increase over the fan; and
η_{fan} = The efficiency of the fan and its electric motor.

Because heat losses in exchangers are neglected, the amount of heat added to water is equal to that which is extracted from the working fluid.

$$\dot{m}_{wf}\left(h_{wf,cond,in} - h_{wf,cond,out}\right) = \dot{m}_{cw}C_{p,cw}\left(T_{cw,out} - T_{cw,in}\right) \tag{46}$$

Pump:
Using the same assumptions that were used for the turbine, power consumed by the feed pump can be calculated as:

$$W_p = \dot{m}_{wf}\left(h_5 - h_4\right) = \dot{m}_{wf}\left(\frac{h_{5s} - h_4}{\eta_p}\right) \tag{47}$$

where η_p is the isentropic pump efficiency and state $5s$ corresponds to an ideal isentropic pump.

Net power output:
Net power output of the power plant, also known as power output, can be calculated by subtracting all auxiliary power requirements from the gross power produced by the turbine.

$$W_{net} = W_t - \left(W_{fan} + W_p\right) \tag{48}$$

The most common and widely used working fluids are hydrocarbon based fluids such as isopentane or propane. A good design and selection of a working fluid gives optimal efficiency, both technically and economically for a given geothermal fluid condition.

5.2 Working fluids

Power plants for generating electricity from hydrothermal resources can be divided into two types: binary and steam. As the word "binary" indicates, there are two cycles in binary plants. The two cycles in such plants are the primary cycle, with the geothermal fluid, and the secondary cycle with the working fluid. The most commonly used fluids are refrigerants and hydrocarbons and, in some cases, a mixture of the two. The Kalina binary power plant is the best example, using a mixture of ammonia and water as a working fluid. The choice of the working fluids depends mainly on the thermodynamic properties of fluids, as well as considerations of health, safety and environmental impacts (DiPippo, 2008).

TABLE 12: Thermodynamic properties of one of the candidate working fluids for binary plants (DiPippo, 2008)

Working fluid	Formula	Crit. temperature (°C)	Crit. pressure (kPa)
Isopentane	i-C_5H_{12}	187.80	3,409

This study only considers isopentane as a working fluid, and the thermodynamic properties of the geothermal brine and boundary conditions. See Table 12 for the thermodynamic properties of isopentane.

6. SYSTEMS MODELLING

6.1 Single-effect water-ammonia absorption system

A single-effect absorption refrigeration technology, water-ammonia absorption refrigeration, is selected for modelling. A single geothermal well feeds the system directly as the heat source, while a machine refrigerates a stream of water for a specific cooling load. The performance of this machine is analysed with variable system components to achieve the best performance. This model is calculated and analysed based on steady state conditions, with the assumptions:

- Heat exchanger is well insulated from the surroundings;
- Potential and kinetic energy changes during heat exchange and at all fluid streams are ignored;
- Modelling the absorption refrigeration system using a geothermal heat source is done by Engineering Equation Solver (EES).

6.2 Absorption refrigeration system description and mathematical modelling

Geothermal fluids for heating a NH_3-H_2O solution have the following technical specifications, as shown in Table 13. Geothermal hot water at 150°C, 30 bar was used in this study under the following two scenarios.

- Power generation in binary cycle where part of the power produced is used to run compressors in a vapour compression refrigeration; and
- Heat production to run a vapour absorption refrigeration cycle.

TABLE 13: Initial design parameters for single-effect ARS

T_{source}	150°C
$\dot{m}_{source}$	3.8 kg/s
Q_{ref}	140 kW
η_{pump}	0.95
η_{she}	0.60
ΔT_{pinch}	5°C
$\Delta T_{evaporator}$	5°C
$T_{condenser}$	38.9°C
$T_{absorber}$	25°C
P_{high}	15 bar
P_{low}	2 bar
$T_{reinjection}$	114.4°C
$T_{cond\ inlet}$	25°C
$T_{cond\ outlet}$	33.9°C

A typical water–ammonia absorption refrigeration system (ARS) is illustrated in Figure 8. The system includes a generator, an absorber, a condenser, an evaporator, and a solution heat exchanger. The determination of the thermodynamic properties of each state point in the cycle, the amount of heat transfer in each component, and the flow rates at different lines, depend upon the generator temperature, evaporator temperature, condenser temperature, absorber temperature, liquid-liquid heat exchanger effectiveness, and the refrigeration load.

A single effect absorption refrigeration system, complete with a solution heat exchanger, is modelled for a water-ammonia system.

In this refrigeration system, the absorption machine provides a cooling effect for the cold storage room with a refrigeration load of 140 kW refrigeration/evaporator capacity. It was assumed that the absorption machine was fed by 150°C geothermal brine from a well at a pressure of 30 bars. The effect of the solution concentration on refrigeration performance is obtained by monitoring the strong and weak concentration differences in a certain range. It was assumed that the generator produced ammonia refrigerant with an ammonia concentration of 99.9 %. A complete list of initial design parameters is displayed in Table 13. Other parameters were freely figured to achieve a preferable machine performance.

6.3 Simulation results of vapour absorption cycle

Table 14 shows the main parameters that were monitored during the analysis of the cycle.

TABLE 14: Heat transfer rates of the system, COP, power consumption and required mass flow

Components	Duty
Generator (Q_g)	295.9 kW
Condenser (Q_c)	215.5 kW
Absorber (Q_a)	221.7 kW
Q_{ref}	140 kW
COP	0.471
Total power required (W-equivalent heat)	91.57 kW
Required mass flow	3.8 kg/s

TABLE 15: Inputs and output parameters for the cycle

Parameters	Compression cycle
Condenser inlet temperature	25°C
Condenser outlet temperature	33.59°C
Pressure high	7.7 bar
Pressure low	2.4 bar
Compressor work	28.12 kW
Electrical power consumed	29.86 kW
COP	4.688

6.4 Simulation results for vapour compression cycle

The thermodynamic properties of the system at various state points (refer to Appendix I, Table 1) were calculated using R134a as a refrigerant by using the equations presented in Table 11. The results given in Table 15 were analysed at $T_3 = 30°C$ and at $T_4 = -5°C$, which are the condenser and evaporator temperatures, respectively. The thermodynamic properties of the state points for a compression refrigeration cycle are shown in Appendix I, Table 1.

6.5 Binary cycle integrated with compression refrigeration

Cooling systems are of different kinds depending on the source of the heat/energy being used to run the cycle. There are heat driven systems, ARS, which are said to be the most effective systems, especially when coupled with refrigeration systems. The design of heat operated systems can be based on different principles. Consider the combination of a (heat operated) binary power station and an electrically operated vapour compression system for refrigeration (Figure 13). On the whole, the combination represents a heat operated system: the primary energy source for operation is the heat supplied in the power station. In Figure 13, it is obvious that there is one "power generating process" and one "refrigeration" process in the system. There are different ways to combine the cycles or to integrate the processes with one another. An obvious combination (from Figure 13) is to build a "double loop system"based on two Rankine cycles. However, the most common example of a heat operated system is the absorption cycle, based on the principle of Carré where the moving part of such a system is, in principle, a liquid pump. This system has some general comments on the coefficient of performance, COP_h of heat operated systems. We can define the COP_h as the ratio between the achieved refrigeration capacity, Q_2, and, necessary heating energy for its operation, Q_b,(shown in Figure 13).

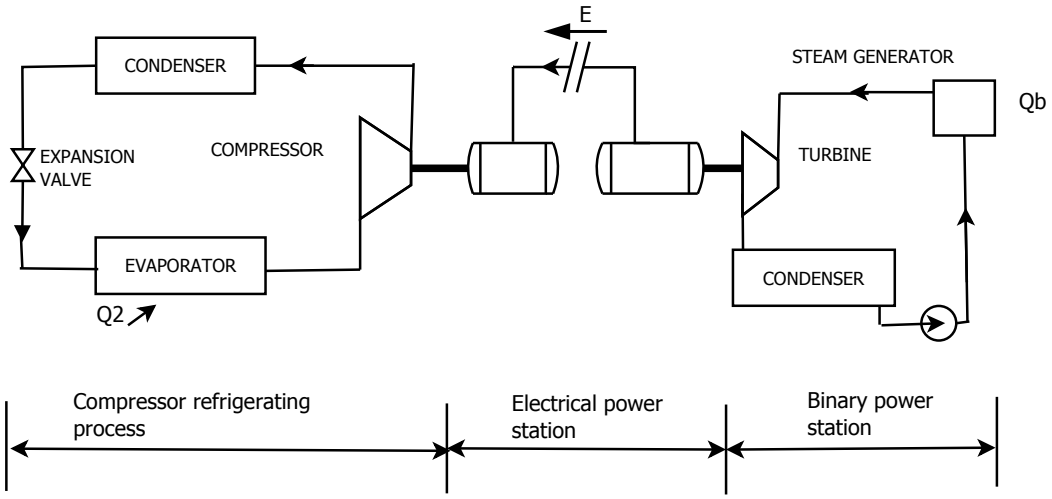

FIGURE 13: A vapour compression refrigeration plant coupled to a binary cycle

$$COP_h = \frac{Q_2}{Q_b} \quad (49)$$

Notice that this relationship differs from that used in the definition of the COP_2, of the regular vapour compression cycle, by that fact that it defines the ratio between two terms expressing "heat energies". Returning to the example given in Figure 13, the COP_h includes not only the refrigeration system, but also the efficiency of the power station. Let us use the symbol η_t for the overall power station and COP_2 for the coefficient of performance of the refrigerating system. It is obvious that the following relationship must prevail.

$$COP_h = \eta_t * COP_2 \quad (50)$$

The COP_h of a heat operated system can always be expected to be smaller than the COP_2 of a system which is based on mechanical (electric) energy for the operation. This observation also implies that, for a given cooling capacity, the heat operated system must be equipped with heat exchangers of larger capacities than a mechanically operated system. This is also an indication that a heat operated system may become more costly to build than an electrical system of the same capacity. However, this comparison is sensitive to the ratio between the cost of an electric motor and compressors in comparison to the heat exchangers (Granryd et al., 2005).

The basic idea of this integrated system was to have a closed loop system for binary power plant power generation where part of it will be used to drive the compression cycle for refrigeration purposes. The integrated system would utilize the heat from a liquid-dominated geothermal well of 150°C geothermal fluid temperature, which is enough to operate a binary cycle geothermal power plant. The system was set to run in a tropical country which has a 25°C ambient temperature.

6.5.1 Binary cycle simulation results

Table 16 shows the simulation results for the thermodynamic properties and heat transfer rates of each component, respectively (refer to Appendix I, Table 2). In this simulation, calculations were performed for a 140 kW cooling load. The results are mostly based on the parameters that were being monitored which are turbine power output, fan and pump inputs and a few others, as shown in Tables 16 and 17.

TABLE 16: Inputs and outputs for binary cycle

Input parameters	Units	Values	Output parameters	Units	Values
Isopentane as working fluid			Net power output	kW	29.86
Mass of the brine	kg/s	0.9	Pump and fan input	kW	1.6
Mass of the working fluid	kg/s	0.52	Thermal efficiency (η_{th})		0.1282
Reservoir temperature	°C	150			
Reservoir pressure	bar	30			

TABLE 17: Comparison between an integrated binary cycle with compression refrigeration and an absorption refrigeration cycle

Input parameters to the cycle	Integrated binary cycle coupled to vapour compression refrigeration	Stand-alone absorption refrigeration system
Thermal power required to run cycle	323.8 kW	295.9 kW
Mass flow of the brine	0.911 kg/s	1.947 kg/s
Re-injection temperature	89.84°C	114.4°C
COP	0.432	0.471

6.5.2 Comparison between integrated binary cycles with compression refrigeration and absorption refrigeration processes

The comparison between these two cycles was mainly based on the efficiency, the thermal power required to run the cycle, the mass flow rates and re-injection temperatures. Basing such a comparison on COP only can sometimes be misleading, as the heat that can be extracted from geothermal brine in a binary cycle is much higher than the heat extracted by the generator in an absorption cycle; other parameters were also compared.

6.6 Discussion on the results

In this simulation process, three cycles, a binary cycle, a compression cycle and an absorption cycle, were analysed. Using input parameters, the thermodynamic properties at the various state points, the energy flow rate at various components of the cycles, the coefficient of performance and the mass flow rates of the system were calculated through the mathematical model by Engineering Equation Solver Software (EES). The results of the EES model are shown in Figures 1-3 in Appendix II. Latent heat of refrigerants and the heat requirement to increase the solution temperature are the main factors that affect the performance of a refrigerant. It was revealed that the absorption refrigeration system should be properly designed to achieve its maximum performance; different amounts of a heat source and cooling loads affect refrigeration parameters. It is also very important to mention that the higher the temperature of the heat source, the better the COP. Also, the efficiency of an absorption machine quickly deteriorates as soon as the temperature of the heat source drops below the design temperature.

7. CONCLUSIONS

The results from the comparison done between a binary cycle integrated with compression refrigeration and vapour absorption refrigeration cycles, for a heat load of 140 kW cold storage, indicate that the binary cycle coupled with compression refrigeration has a lower COP of 0.432**,** compared to 0.471 for the absorption cycle. Also, the geothermal fluid mass flow required to drive the absorption cycle is higher than that required to drive a binary cycle coupled to a compression cycle for the same cooling effect. The thermal power required to drive the binary cycle is 323.8 kW, while that of an absorption cycle is 295.9 kW**,** which combines the power required for the pump work done by the absorber, condenser and evaporator.

8. RECOMMENDATIONS FOR FUTURE WORK

Changing more variables in the optimization process is one possibility in order to achieve a higher system performance. In a binary cycle, this can be applied by varying the well head pressure. By changing this pressure, especially if different mass flows are applied, the system performance can be further optimized. For the absorption refrigeration cycle, the addition of a separator (rectifier) to the cycle may be worked on to increase system efficiency. An overview of system performance based on exergetic efficiency could be analysed to measure the potential work and final work output relative to environmental conditions. Finally, the economic performance of absorption chillers could be analysed, even if it is known that a heat operated system (chillers) may become more costly to build than an electrical system of the same capacity due to more components of the cycle; such a comparison would be sensitive to the ratio between the cost of an electric motor and compressors in comparison to the heat exchangers.

ACKNOWLEDGEMENTS

This is a great opportunity to express my respect for all those who aided me in completing this six month program. I am pleased to thank the Government of Iceland through the United Nations University for the financial support. My gratitude goes to Mr. Lúdvík S. Georgsson, the director of UNU-GTP, for the fellowship, and Dr. Ingvar Birgir Fridleifsson, the outgoing director; also to all the UNU-GTP staff, Mr. Ingimar G. Haraldsson, Ms. Thórhildur Ísberg, Ms. Málfridur Ómarsdóttir and Mr. Markús A. G. Wilde, for their continuous help. I am very grateful to my advisors, Mr. Thorleikur Jóhannesson and Mr. Davíd Örn Benediktsson, for encouraging and supervising me. Thank you for the time and the discussions. I also would like to extend my appreciation to all staff and lecturers of Orkustofnun and Iceland GeoSurvey - ÍSOR, for sharing their experience with us. I would also like to thank all the UNU Fellows for our memorable time and friendship.

This report is especially dedicated to my parents and my family, in general; thanks for the moral support, prayers and care.

REFERENCES

Agri, 2012: *Knowledge centre*. Banque Populaire, Rwanda, Ltd.

ASHRAE, 2009: *ASHRAE handbook - Fundamentals*. American Society of Heating Refrigerating and Air-conditioning Engineers, Atlanta, GA, United States, 880 pp.

Bäckström, M., 1970: *Kylteknikern* (in Swedish). Svenska kyltekniska föreningen, 928 pp.

BGR, 2009: *Geothermal potential assessment in the Virunga geothermal prospect, Northern Rwanda.* Federal Institute for Geosciences and Natural Resources (BGR), final report, 104 pp.

DiPippo, R., 2008: *Geothermal power plants. Principles, applications, case studies and environmental impact*. Elsevier Ltd., Kidlington, United Kingdom, 493 pp.

Granryd, E., Ekroth, I., Lundqvist, P., Melinder, A., Palme, B., and Rohlin P., 2005: *Refrigerating engineering.* Stockholm.

Hauksson, Th., 2013: *Utilization of absorption cycles for Nesfiskur and Skinnfiskur.* University of Iceland, Reykjavík, MSc thesis, 97 pp.

Lukawski, M., 2009: Design and optimization of standardized organic Rankine cycle power plant for European conditions. RES - the School for Renewable Energy Science in affiliation with the University of Iceland and the University of Akureyri, Akureyri, MSc thesis, 87 pp.

Namugize, J.N., 2011: Preliminary Environmental Impact Assessment of geothermal exploration and development in Karisimbi, Rwanda. Report 28 in: *Geothermal training in Iceland 2011*. UNU-GTP, Iceland, 669-708.

Newell, D., Rohrs, D., and Lifa, J., 2006: *Preliminary assessment of Rwanda's geothermal energy development potential*. Chevron Corporation, Indonesia, report, 27 pp.

NISR, 2012: *Statistical yearbook, 2012*. National Institute of Statistics, Rwanda, 187 pp.

Onacha S.A., 2008: *Geothermal resources exploration programme in Rwanda.*

Onacha S.A., 2011: Rwanda geothermal resources development, country update. *Proceedings of the Kenya Geothermal Conference KGC 2011, Nairobi*, 6 pp.

PalletLink, 2013: *Storage box design*. PalletLink, website: *www.palletlink.com/potato-boxes/box-design/*

Planck, R., and Niebergall, W., 1959: *Handbuch der Kältetechnik: Sorptions-Kältemaschinen, 7.* Springer Verlag, Berlin, Germany, 559 pp.

Ratlamwala, T., Dincer, I., and Gadalla, M.G., 2012: Thermodynamic analysis of a novel integrated geothermal based power generation-quadruple effect absorption cooling-hydrogen liquefaction system. *Internat. J. Hydrogen Energy, 37-7,* 5840–5849.

Soslow, T.V., Trevor, V., and Voss, R., 2013: *Potato – recommendations to maintain post harvest quality* (in French). UC Davis, website: *postharvest.ucdavis.edu/L%C3%A9gumes/Pomme_de_Terre/*

Southern California Gas Company New Buildings Institute, 1998: *Absorption chillers.* Advanced Design Guideline Series, 97 pp.

Srikhirin, P., Aphornratana, S., and Chungpaibulpatana, S., 2001: A review of absorption refrigeration technologies. *Renewable and Sustainable Energy Reviews, 5*, 343-372.

Tesha, 2009: Abs*orption refrigeration system as an integrated condenser cooling unit in a geothermal power plant*. University of Iceland, MSc thesis, UNU-GTP, Iceland, report 1, 68 pp.

Wulfinghoff, D.R. 1999. *Energy efficiency manual*. Energy Institute Press, 1536 pp.

APPENDIX I: Thermodynamic graphs and properties

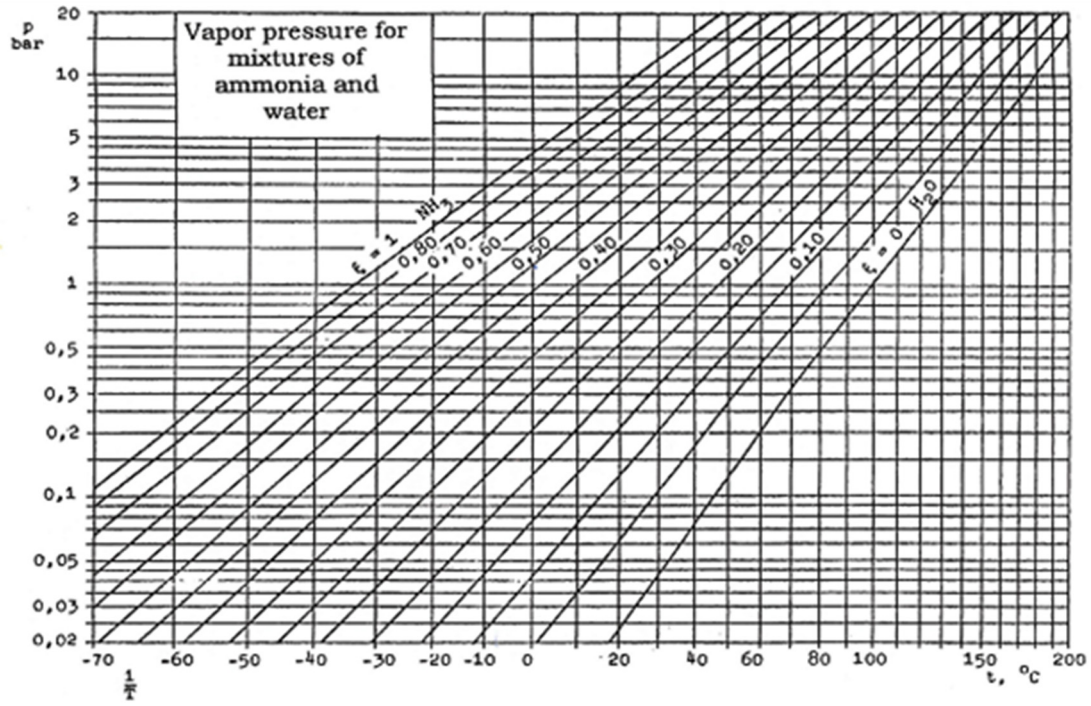

FIGURE 1: Saturation vapour pressure of NH_3-H_2O solutions
(data from Planck and Niebergall,1959)

TABLE 1: Thermodynamic properties of state points for the compression refrigeration cycle shown in Figure 9

State points	Specific enthalpy (kJ/kg)	Pressure (bar)	Specific entropy (kJ/kg K)	Temperature (°C)	X (%)
1	247.5	2.435	0.9344	-4.99	100
2	275.6	7.706	0.948	38.59	100
3	93.58	7.706	0.3479	30	0
4	93.58	2.435	0.3603	-5	0.2392

TABLE 2: Thermodynamic properties of state points for the absorption refrigeration cycle shown in Figure 8

State points	Specific enthalpy (kJ/kg)	Mass flow rate (kg/s)	Pressure (bar-a)	Specific entropy (kJ/kg K)	Temperature (°C)	Concentration (x)
1	-64.89	0.6356	2	0.4013	35	0.3678
2	-62.74	0.6356	15	0.4013	35.08	0.3678
3	301.9	0.6356	15	1.452	109.4	0.3678
4	491.2	0.5057	15	1.822	145	0.2056
5	32.84	0.5057	15	0.5627	40.08	0.2056
6	32.84	0.5057	2	0.5673	40.35	0.2056
7	1842	0.1299	15	5.523	145	0.999
8	183.6	0.1299	15	0.6396	38.87	0.999
9	183.6	0.1299	2	0.7464	-18.67	0.999
10	1261	0.1299	2	4.959	2.516	0.999

APPENDIX II: Results of EES simulations

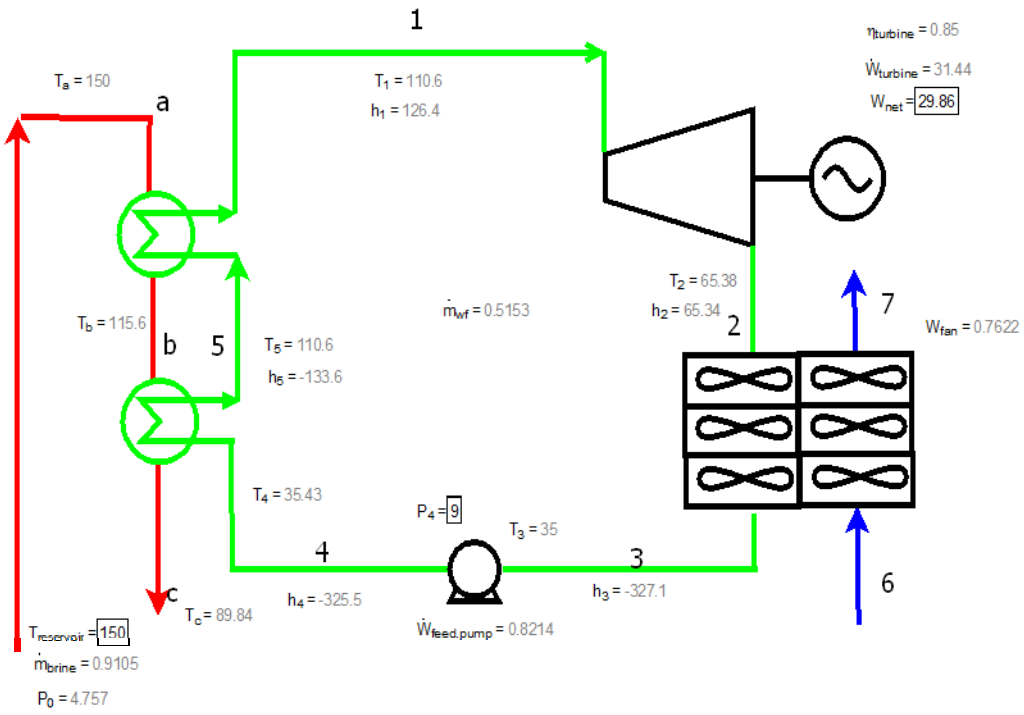

FIGURE 1: ORC power plant, EES simulation

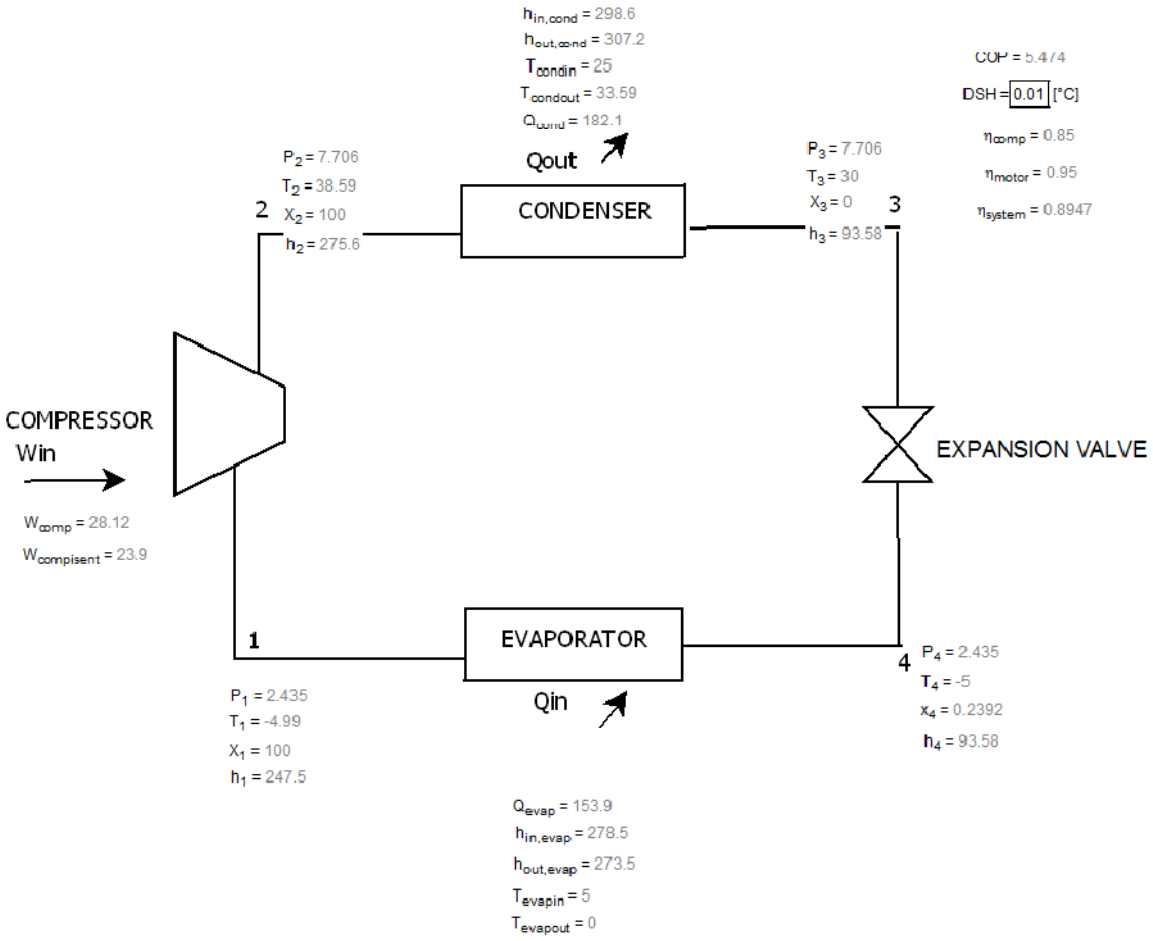

FIGURE 2: Compression cycle, EES simulation

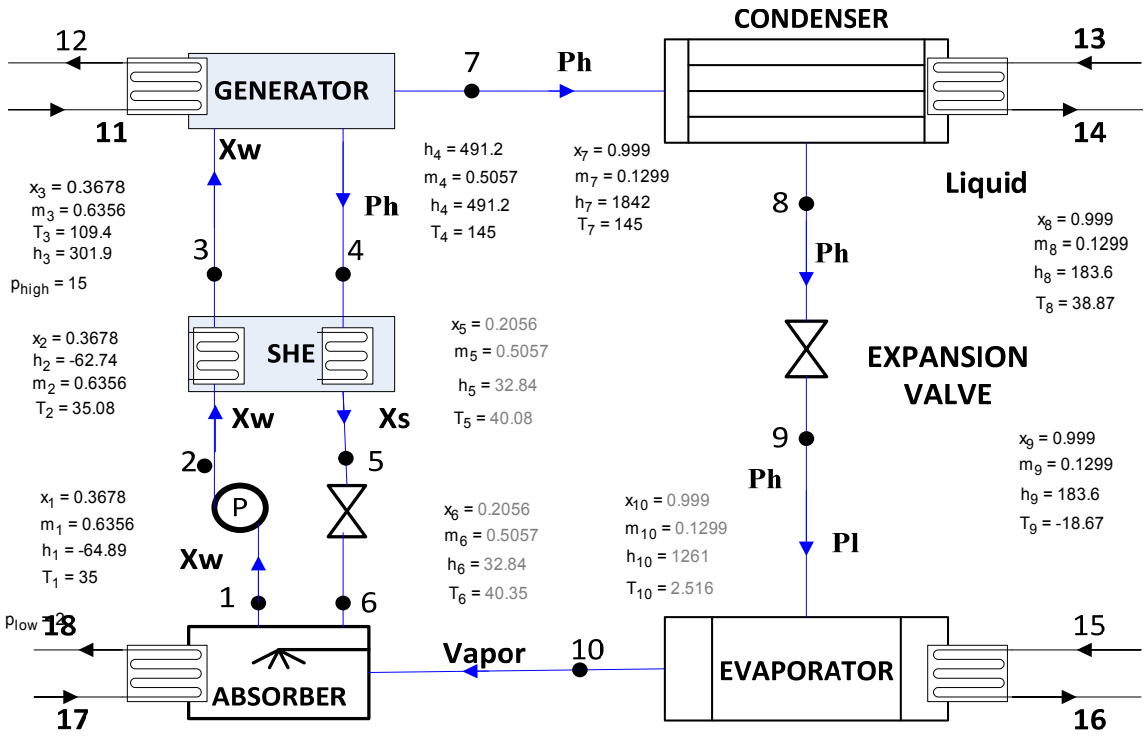

FIGURE 3: Absorption cycle, EES simulation